Solution Structure of the C-Terminal Transcriptional Activator Domain of FixJ from *Sinorhizobium meliloti* and Its Recognition of the *fixK* Promoter[†,‡]

Kaori Kurashima-Ito,[§] Yuichi Kasai,[§] Kaito Hosono,[||] Koji Tamura,[⊥,#] Soichi Oue,[▽] Miho Isogai,[▽] Yutaka Ito,[§,⊥,#] Hiro Nakamura,[§,○] and Yoshitsugu Shiro*[,○]

Yokohama City University, Suehiro, Tsurumi, Yokohama, Kanagawa 230-0045, Japan, RIKEN Harima Institute, Mikazuki, Sayo, Hyogo 679-5148, Japan, RIKEN, Wako, Saitama 351-0198, Japan, Hosei University, Koganei, Tokyo 184-8584, Japan, and Gakushuin Univerisity, Mejiro, Toshima, Tokyo 170-0031, Japan

Received May 15, 2005; Revised Manuscript Received August 27, 2005

ABSTRACT: FixJ is a response regulator of the two-component signal transduction pathway involved in the transcriptional activation of nitrogen fixation genes of *Sinorhizobium meliloti*. Upon phosphorylation, FixJ transcriptionally activates the *fixK* and *nifA* promoters. We identified a FixJ recognition sequence of 16 bp in the high affinity binding site of the *fixK* promoter by means of a gel shift assay. In addition, the solution structure of the truncated C-terminal DNA binding domain of FixJ (FixJC) was solved by NMR spectroscopy. FixJC contains five α-helices that encode a typical helix−turn−helix motif as a potential DNA binding core with the highest structural similarity toward the C-terminal DNA binding domain of NarL. The addition of the DNA fragment containing the recognition sequence of the high affinity FixJ binding site resulted in intermediate to slow exchange interactions on the NMR time scale in the spectrum of FixJC, while the exchange was rapid in the case of control DNA. These spectral data suggest that more than one molecule of FixJC binds to the recognition sequence, although FixJC alone is present in monomeric form in solution. This result is consistent with a scenario in which a transcriptionally active species of FixJ is a homodimer of the phosphorylated form.

Rhizobial FixL and FixJ proteins have been genetically identified as oxygen-sensing components that direct the expression of genes that are involved in symbiotic nitrogen fixation in hypoxic root nodules in host plants (*1*). The nucleotide sequence indicates that they are a sensory histidine kinase, along with its cognate response regulator, and are members of the superfamily of bacterial two-component signal transducing systems. At low oxygen tension, oxygen-free FixL is autophosphorylated by ATP at an invariant histidine residue, and the phosphoryl group is transferred to a conserved Asp residue of FixJ, while the oxygen-bound form reduces the histidine kinase activity at high oxygen tension (*2*).

FixJ consists of an N-terminal receiver domain and a C-terminal effector domain. The acceptance of the phosphoryl group at Asp54 of the receiver domain from FixL enhances its transcriptional activator function, i.e., the DNA binding ability of the effector domain toward the promoter regions of the target genes, *fixK* and *nifA* (*3*, *4*). Since FixJC[1] exhibits binding to these promoters, the unphosphorylated N-terminal receiver domain appears to exert an inhibitory effect within the full-length protein, which is relieved upon phosphorylation and concomitant dimerization (*5*, *6*). Because of the high similarity in the amino acid sequence of FixJC with the C-terminal DNA binding region of another response regulator, NarL (*7*) (Figure 1), the DNA binding of FixJ is thought to be similar to that of NarL. However, the mechanisms by which their DNA binding domains are activated remain to be elucidated at an atomic resolution.

The C-terminal domain of FixJ is expected to contain an HTH motif similar to NarL and Spo0A, although the DNA sequences of the target promoters are different from each other (*8*, *9*). Thus, another issue to be solved is how the individual response regulators recognize their own target promoters. It is also noteworthy that the *nifA* and *fixK* promoters share no sequence homology, and neither significant tandem nor palindromic sequences are present in these promoters (*10*) although the dimeric form of phosphorylated FixJ binds to them (*6*). Such differences in DNA sequence between the two promoters suggest that phosphorylated FixJ binds to these promoters but that the nature of the binding is unique for each promoter. However, no structural evidence for this has yet been reported.

[†] This work was supported, in part, by the Bioarchitect Research in RIKEN, and a Grant-in-Aid for Scientific Research of Priority Areas on Metal Sensors (No. 12147210) from the Ministry of Education, Culture, Sports, Science and Technology of Japan to H.N.

[‡] PDB file name: 1X3U.

* Corresponding author. Tel: 81 (791) 58 2817. Fax: 81 (791) 58 2818. E-mail: yshiro@riken.jp.

[§] Yokohama City University.

[||] Hosei University.

[⊥] RIKEN, Wako.

[#] Present addresses: K.T., Scripps Institute, La Jolla, CA 92037; Y.I., Tokyo Metropolitan University, Minami-Osawa, Hachioji, Tokyo 192-0397, Japan.

[▽] Gakushuin Univerisity.

[○] RIKEN Harima Institute, Mikazuki, Sayo.

[1] Abbreviations: FixJC, the truncated C-terminal domain of FixJ; HTH, helix−turn−helix motif; IPTG, isopropyl β-D-thiogalactopyranoside; PMSF, phenylmethanesulfonyl fluoride; Ni-NTA, nickel nitrilotriacetic acid; CM, carboxymethyl; CSI, chemical shift index; FixJ−P, the phosphorylated form of FixJ.

10.1021/bi0509043 CCC: $30.25
Published on Web 10/19/2005

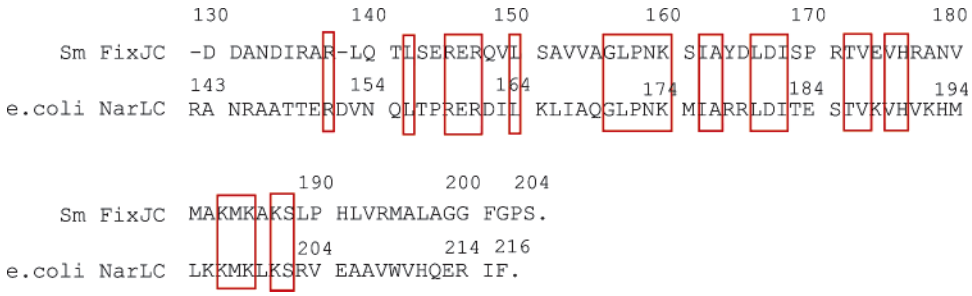

FIGURE 1: Amino acid alignment of the DNA binding domains of FixJ and NarL. Identical amino acids between the two are boxed.

In the present study, we identified the essential sequence of the *fixK* promoter for FixJ binding and determined the solution structure of FixJC, in an attempt to understand the binding interaction between the promoter and FixJC using NMR spectroscopy. The results suggest that two molecules of the active FixJ species synergistically bind in a specific and nonspecific manner with a rather low binding affinity.

MATERIALS AND METHODS

Gel Shift Assay of the FixJ−fixK Promoter Complex. Preparation of the FixJ protein and its phosphorylation with acetyl phosphate were carried out as previously described (*11*). The FixJ−DNA complexes were formed by incubating 15 μM FixJ and 0.33 μM DNA in 89 mM Tris borate pH 8.0, 2 mM Na-EDTA, 1.7 mM $MgCl_2$ at room temperature for 30 min. Fifteen microliter aliquots of the solution were applied to a 10% polyacrylamide gel in 89 mM Tris borate pH 8.0, 2 mM Na-EDTA. The electrophoresis was carried out at 50 V × 3.3 h in the cold (4 °C). The DNAs separated in the gels were visualized using a GelStar stainer (Bio-Whittaker Molecular Applications).

Expression and Protein Purification of FixJC for NMR Experiments. For the expression of FixJC, the DNA corresponding to Asp130−Ser204 accompanied by the *Nde*I and *Bam*HI sites was subcloned into pET-14b (Novagen), and the resulting expression plasmid was introduced into *Escherichia coli* strain JM109 (DE3).

Uniformly $^{13}C/^{15}N$ labeled FixJC protein was obtained by growing the transformed bacteria at 37 °C in M9 minimal medium containing 0.5 g/L $^{15}NH_4Cl$ and 2 g/L [$^{13}C_6$] D-glucose as the sole nitrogen and carbon sources, respectively. At an $OD_{600\ nm}$ of ∼0.8, protein expression was induced by the addition of IPTG to a final concentration of 1 mM. After 4 h of further growth at 37 °C, the cells were harvested, washed, and stored at −80 °C.

All the purification procedures described below were carried out at 4 °C. The cell pellet was suspended in buffer A [50 mM potassium phosphate (pH 7.5), 150 mM NaCl, 5% glycerol, 5 mM β-ME, 20 mM imidazole, 1 mM PMSF]. Lysis was performed by two passages of a French press after lysozyme treatment (0.1 mg/mL). The cell debris was clarified by centrifugation at 64000*g* for 60 min. The 6xHis-tag FixJC was purified by chromatography on a Ni-NTA affinity column (QIAGEN). Cleavage of the 6xHis-tag was achieved by thrombin digestion, followed by passage of the solution through the Ni-NTA to remove the cleaved tag. FixJC-containing fractions were then loaded onto a CM-Sepharose fast flow cation exchange column preequilibrated with buffer B [20 mM Tris-HCl, 10 mM β-mercaptoethanol] and eluted using a NaCl gradient. The final FixJC fractions were collected and concentrated. This FixJC sample has four vector-derived extra residues (GlySerHisMet) at the N-terminal of the protein.

NMR Spectroscopy. Purified $^{13}C/^{15}N$-labeled FixJC was dissolved in NMR buffer [90% ^1H_2O/10% ^2H_2O containing 20 mM $NaHPO_4-NaH_2PO_4$ (pH 5.5), 100 mM NaCl, 50 mM Na_2SO_4] and concentrated (∼1 mM). All NMR experiments were performed at a probe temperature of 25 °C on a DRX-600 spectrometer. All spectra were processed on LINUX-PCs with the Azara 2.6−2.7 package (W. Boucher, unpublished, http://www.bio.cam.ac.uk/azara/). For the 3D data, the two-dimensional maximum entropy method (*12*) was applied to obtain resolution enhancement for indirect dimensions. All of the spectra were analyzed on LINUX-PCs with the combination of customized macro programs on the OpenGL version of ANSIG 3.3 software (*13*).

For backbone $^1H^N$, ^{15}N, $^{13}C^\alpha$, and $^{13}C'$ and side-chain $^{13}C^\beta$, resonance assignments were achieved by analyzing spin−spin connectivities in four types of 3D triple-resonance experiments, CBCA(CO)NH (*14*), CBCANH (*15*), HNCO (*16*), and HN(CA)CO (*16*). The following were used for the resonance assignment of the side-chain ^1H and ^{13}C resonances: 3D experiments of HBHA(CO)NH (*17*), H(CCCO)-NH (*18*, *19*), (H)CC(CO)NH (*19*), and HCCH-TOCSY (*20*). The side-chain NH_2 group assignment was achieved by collecting another (H)CC(CO)NH spectrum, in which the delays were optimized for observation of NH_2 groups. The assignments of $^1H^\epsilon-^{15}N^\epsilon$ of arginine and side chains of aromatic residues were achieved by analyses of ^{15}N- and ^{13}C-separated NOESY-HSQC spectra (*21*) with a mixing time of 150 ms, respectively.

Structure Calculation. 3D ^{15}N-separated and ^{13}C-separated NOESY cross-peaks were selected and unambiguously assigned wherever possible. For each spectrum, the "connect" program within AZARA package was used to convert normalized peak intensities into four distance categories of <2.7, 3.3, 5, and 6 Å. Two separate lists, one of unambiguous NOE restraints, the other of ambiguous restraints, were then produced by the "connect", allowing 0.04 and 0.3 ppm tolerance for errors in the ^1H and $^{15}N/^{13}C$ dimensions, respectively. Hydrogen bond derived distance constraints were obtained from an analysis of the slowly exchanging amide protons in the 3D ^{15}N-separated NOESY spectrum. Dihedral angle restraints for backbone ϕ and ψ angles were generated from the calculation of CSI (*22*) using $^{13}C^\alpha$, $^{13}C^\beta$, and $^{13}C'$ chemical shifts. These restraint files were input to CNS (*23*) version 1.1 based procedures and subjected to a simulated annealing protocol using the default NMR force field. Three manual iterative assignment processes were performed on the ambiguous NOEs by eliminating assign-

ment possibilities that contributed less than 1%, 2%, and finally 5%. Twenty structures were selected on the basis of having the lowest NOE-derived energies among the 80 structures calculated. The quality of the final ensemble of the calculated structures was assessed by analyzing Ramachandran plots with PROCHECK (*24*) and deviations in the calculated $^1H^\alpha$ chemical shifts from the observed values with the TOTAL program (*25*, *26*).

NMR Titration of $^{13}C/^{15}N$-Labeled FixJC with Specific and Nonspecific DNA Duplexes. For NMR titration experiments, $^{13}C/^{15}N$-labeled FixJC was dissolved in a titration buffer [20 mM Tris-acetate (pH 6.8), 100 mM NaCl] and concentrarted to 100 μM. Two 21 bp double-stranded DNA fragments, d(GCTAAGTAATTTCCCTTAGTG)/(CACTAAGGGAAATTACTTAGC) and d(GTGATCTAACCCAATTTCTCC)/(GGAGAAATTGGGTTAGATCAC), corresponding to two different regions, −67 to −47 and −49 to −29 regions, respectively, of the *fixK* promoter sequence were synthesized. Two series of 2D $^1H-^{15}N$ HSQC (*27*, *28*) spectra were collected for $^{13}C/^{15}N$-labeled FixJC with various concentrations (0, 12.5, 25, 50, 100, and 200 μM) of the above-mentioned two DNA fragments. During the titration, the total volume was kept constant at 250 μL with titration buffer. For the complete backbone assignment of FixJC on its own under buffer conditions, 3D HNCA, HN(CO)CA experiments (*29*) were measured at 25 °C and analyzed.

RESULTS

Target Sequence of the fixK Promoter for FixJ Binding. It has previously been shown that SmFixJ directs the expression of both the *fixK* and *nifA* genes (*3*, *4*), but that other rhizobial FixJs are involved only in *fixK* gene expression, in which the promoter sequences are partially conserved (*30*). Thus, in the present study, Sm*fixK* promoter was used as a target DNA for FixJ−P binding. A nuclease protection assay indicated that the −69 to −44 region serves as a high affinity binding site, which appears to be responsible for FixJ-dependent regulatory function (*4*). Because DNA protection assays do not permit the recognition sequence to be identified directly, we carried out a gel shift assay for wild-type and mutated DNAs to determine the FixJ recognition sequence (Figure 2).

FixJ specifically binds to the wild-type sequence when it is phosphorylated (Figure 2a). The M1, M2, and M3 mutants were refractory to the binding of FixJ−P, consistent with the fact that $T_{-65}AAG_{-62}$ and $C_{-55}CCTT_{-51}$ are the most conserved among the *fixK* promoters of various rhizobia (*30*). FixJ−P failed to bind to M4, indicating that $A_{-60}ATT_{-57}$ is also required. However, it binds successfully to M5. Finally, a binding assay with a series of consecutively mutated DNAs indicated that the sequence 5′-T_{-56}AAGTAATTTCCCTTA$_{-50}$-3′ is required for FixJ−P to recognize the *fixK* promoter sequence (Figure 2c). We then determined the solution structure of the DNA binding domain of FixJ, and analyzed the interaction between the DNA sequence identified and the FixJC protein.

Structural Determination. FixJC, a truncated protein consisting of residues 130−204 of the C-terminal region, was analyzed by NMR. The nearly complete backbone and side-chain ^1H, ^{13}C, and ^{15}N resonance assignments of FixJC were achieved by analysis of spin−spin connectivities in a

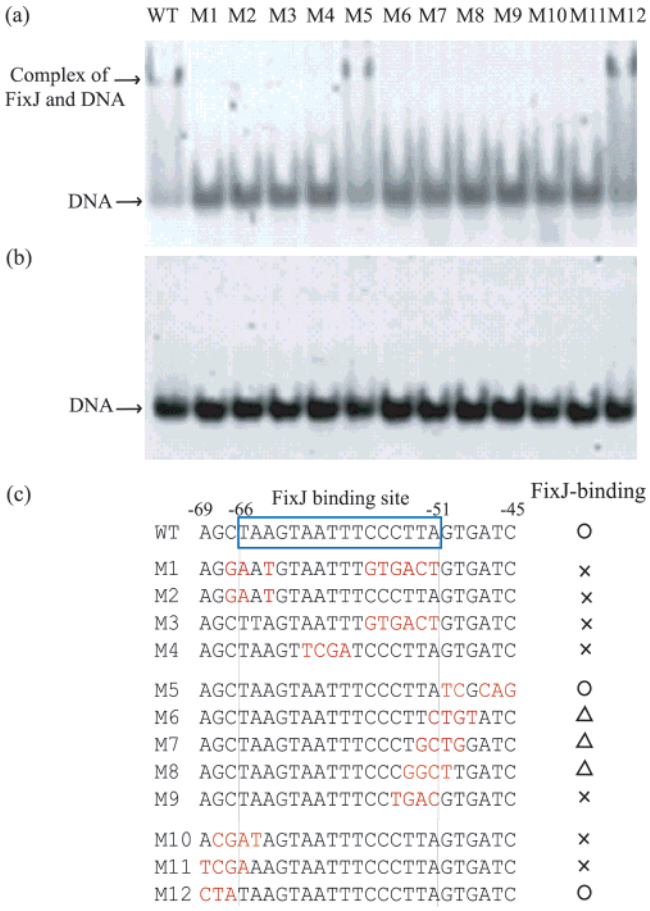

FIGURE 2: Identification of the high affinity binding site of the *fixK* promoter by FixJ−P. Binding of phosphorylated FixJ (a) and unphosphorylated FixJ (b) to various 25 bp double-stranded DNAs derived from the −68 to −44 region of the *fixK* promoter was analyzed by gel retardation assays. The wild-type sequence and 12 mutants were subjected to polyacrylamide gel electrophoresis in the presence of either phosphorylated or unphosphorylated FixJ. The DNA bands were visualized with GelStar stainer. (c) The results are summarized with the corresponding DNA sequences. Elucidated FixJ-binding site on the *fixK* promoter DNA, inferred from the data, is shown as a box on the wild-type sequence. Circle, normal binding similar to the wild-type sequence; cross, failure in binding; triangle, weak binding showing a small amount of supershifts.

series of 3D triple-resonance NMR spectra. The chemical shift assignments are listed in the Supporting Information. The secondary structure of FixJC, predicted by a CSI analysis (*22*) of the assigned $^{13}C^\alpha$, $^{13}C^\beta$, and $^{13}C'$ resonances (Figure 3b), and an analysis of sequential and medium-range NOEs (Figure 3c) showed that this domain consists of five α-helices (Figure 3d).

The solution structure of FixJC was determined from a total of 3121 unambiguous restraints (1604 intraresidue, 771 sequential, 652 medium-range, and 94 long-range distance restraints) and 698 ambiguous restraints, 54 hydrogen bond derived distance restraints, and 53 ϕ/ψ dihedral angle restraints. Figure 3e and Figure 3f show the numbers of unambiguous and ambiguous NOE constraints per residue, respectively. The ambiguous restraints were included in the calculations from the initial stage using a sum-average potential function (*31*). Structural statistics of the final ensemble of 20 refined structures are summarized in Table 1. Figure 4a shows backbone traces of an ensemble of the 20 refined structures superimposed on the backbone C^α, N, C′ atoms.

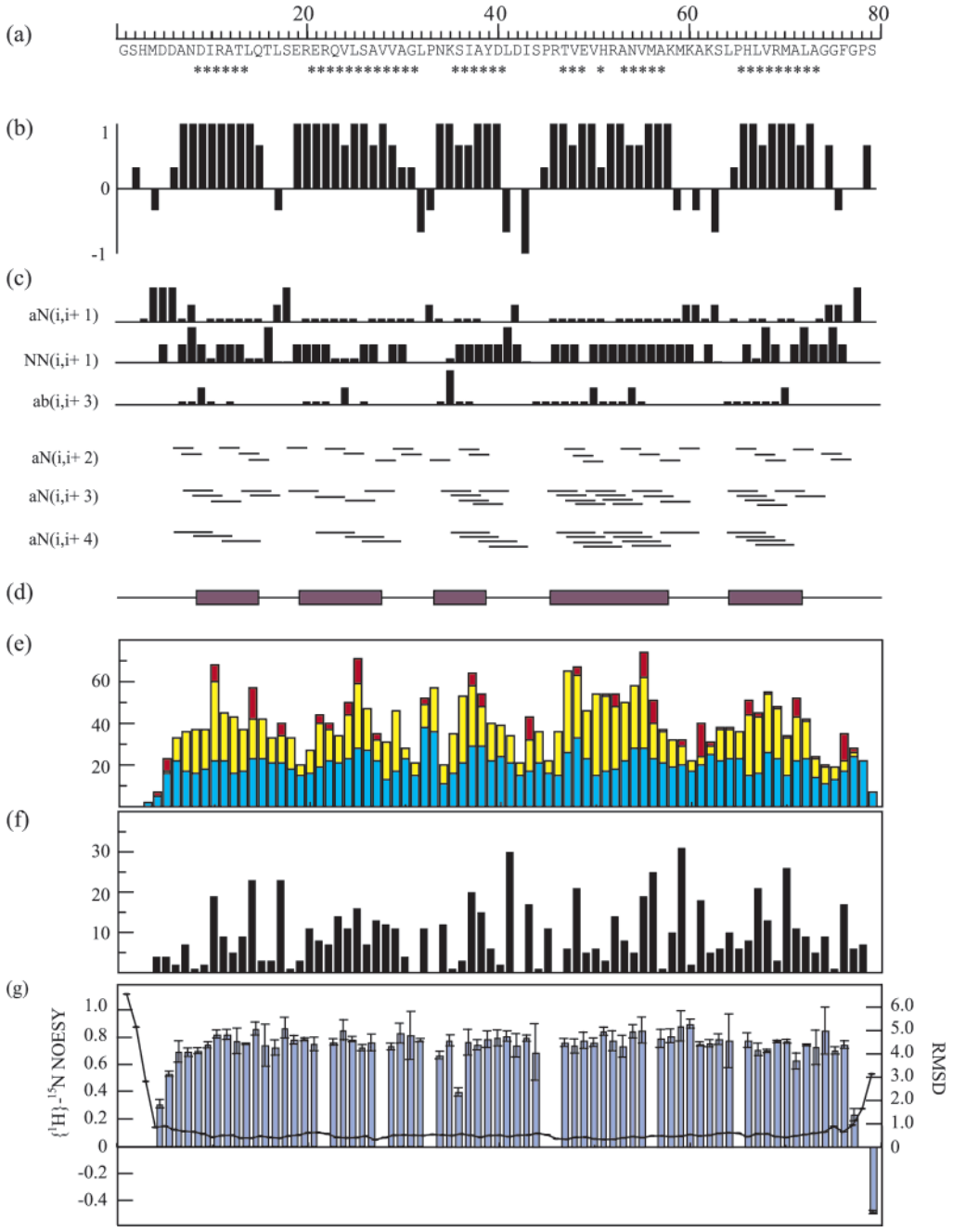

FIGURE 3: Summary of homonuclear and heteronuclear NOEs, CSI, and rms deviations. (a) The amino acid sequence of FixJC. The observed slow exchange of amide protons is indicated by the symbol (*) under the corresponding residues. (b) The consensus CSI_{av} calculated according to the following equation: $CSI_{av} = [(CSI\ ^{13}C^{\alpha} + CSI\ ^{13}C' - CSI\ ^{13}C^{\beta})/3]$. (c) Sequential and short-range NOEs. The height of each block in the sequential NOEs corresponds to the magnitude of the NOEs. (d) Summary of the secondary structure inferred from the data shown in panels a, b, and c. (e) Number of unambiguous NOE-derived distance restraints used in the structure calculations. Blue, yellow, and red bars correspond to sequential ($i \rightarrow i + 1$), medium-range ($i \rightarrow i +$ (2, 3, or 4)), and long-range ($i \rightarrow i +$ (>4)) NOEs, respectively. (f) Number of ambiguous NOE-derived distance restraints used in the structure calculation. (g) $\{^1H\}-^{15}N$ heteronuclear NOEs for the backbone amides (vertical bars) and rms deviation (Å) of the C^{α} atoms for the ensemble of 20 structures.

The backbone structure is well-defined except for three N-terminal vector-derived residues and two C-terminal residues. Analysis of $\{^1H\}-^{15}N$ steady-state NOEs confirmed that the N-terminal and C-terminal regions are flexible (Figure 3g). The rms deviations of the final 20 structures from the average for the backbone C^{α}, N, C′ atoms and all nonproton atoms in residues 4−77 were 0.507 and 1.027 Å, respectively. A ribbon representation of the structure closest to that of the mean of the ensemble (Figure 4b) exhibits a rigid helical bundle of five α-helices, α1(Asp134 to Gln140), α2(Glu144 to Va153), α3(Asn158 to Asp165), α4(Thr172 to Lys183), and α5(Leu189 to Leu197). Among them, α3, α4, and the connecting loop form an orthodox HTH motif.

Structural Comparison with the DNA Binding Domain of NarL. To date, the structures of the DNA binding regions of response regulators have been determined for NarL, OmpR, PhoB, DrrD, Spo0A, PrrA, and RcsB (*32*−*38*). Figure 5a and Figure 5b show a comparison of the structure of FixJC with the C terminal half of the crystal structure of unphosphorylated NarL, which contains four α-helices (α7−α10) and the corresponding region (α2−α5) of the solution structure of FixJC. The rms difference between these two

Table 1: Structural Statistics for the 20 Lowest Energy Structures

	ensemble	closest to mean
no. of NOE restraints:	3819	3819
unambiguous	3121	3121
ambiguous	698	698
for unambiguous NOEs:		
intraresidue	1604	1604
sequential	771	771
medium range ($i - j \leq 4$)	652	652
long range ($i - j > 4$)	94	94
distance restraints for hydrogen bonds	54 (27 hydrogen bonds)	54 (27 hydrogen bonds)
backbone dihedral angle restraints from CSI	53 (ϕ), 53 (ψ)	53 (ϕ), 53 (ψ)
coordinate rmsd (Å):		
all residues		
backbone heavy atoms	1.035	0.620
all heavy atoms	1.371	1.048
residues 4−77		
backbone heavy atoms	0.507	0.396
all heavy atoms	1.040	0.956
parameter rmsd from idealized geometry:		
av NOE restraint violation (Å)	0.0391 ± 0.0016[a]	0.0400
bond length (Å)	0.0036 ± 0.0001[b]	0.0036
bond angles (deg)	0.4630 ± 0.0112[b]	0.4558
Ramachandran assessment (%):		
most favored region	78.3	73.9
additionally favored region	18.6	20.3
generously allowed region	2.8	5.8
disallowed region	0.3	0.0

[a] The sum of the NOE violations divided by the total number of restraints, averaged over the ensemble. [b] The rmsd for each structure, averaged over the ensemble.

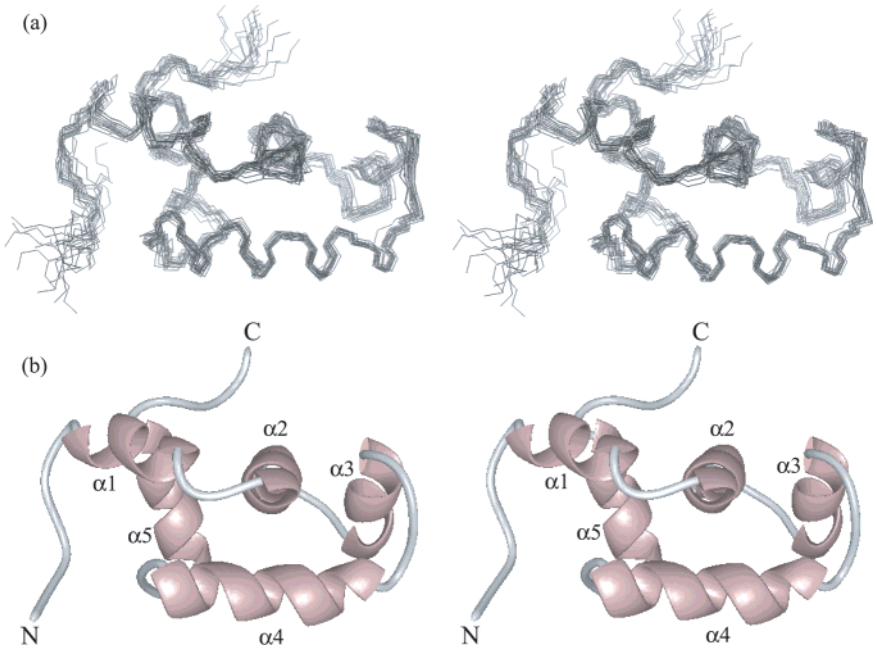

FIGURE 4: The solution structure of the C-terminal domain of FixJ. (a) A stereoplot of the backbone traces of an ensemble of 20 calculated structures superimposed on the backbone heavy atoms. (b) A stereoplot of the ribbon representation of the structure closest to that of the mean of the ensemble in the same orientation as in panel a. The plots were produced using the MidasPlus software from the Computer Graphics Laboratory, University of California, San Francisco.

structures is 1.25 Å for the backbone C^{α} atoms, indicating a high degree of structural similarity. Figure 5c represents the structure of the C-terminal domain of Spo0A, showing that Spo0A shares the common relative orientation of the four α-helices (αA−αF for Spo0A) mentioned above.

A crystallographic study on the NarLC−DNA complex has shown that the first three helices (α7−α9) are responsible for DNA binding (*39*). In particular, the second and third helices are referred to as "scaffolding" and "recognition" helices, respectively, of a classical HTH motif. Several residues, which are directly involved in the DNA binding of NarLC (Figure 6b), were found to be conserved at the identical or proximal positions of FixJC (Figure 6a). Among them, four basic residues, Arg145/Arg159, Lys160/Lys174, His176/His190, and Lys186/Lys201 of FixJC/NarLC, appear to participate in electrostatic interactions with DNA backbone. In contrast, the nonconservative residues of the individual recognition helices may participate in the specific

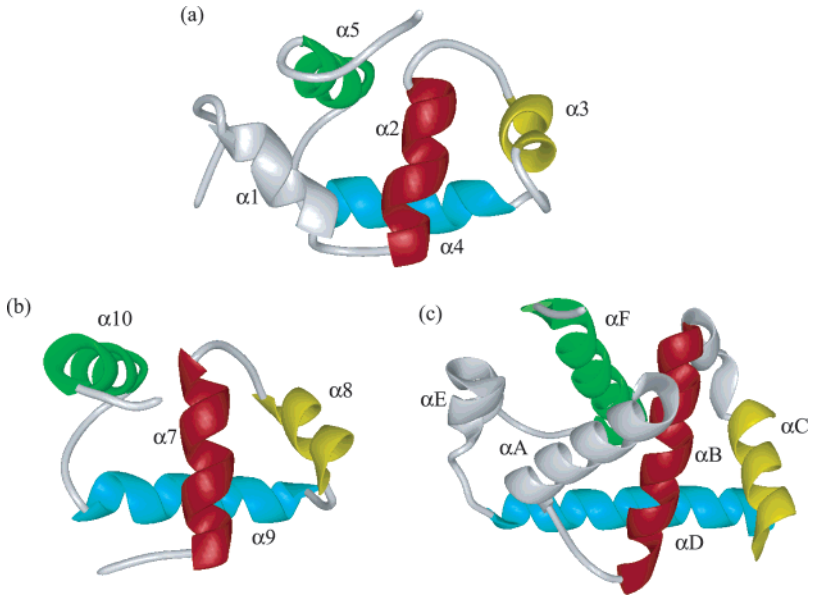

FIGURE 5: Structural comparison of the DNA-binding domains of the response regulators, FixJ (a), NarL (b), and Spo0A (c). In the structures of NarLC and Spo0AC, the helices corresponding to α2, α3, α4, and α5 in FixJC are represented by the same color codes. Cyan and yellow helices indicate the recognition and scaffolding helices, respectively.

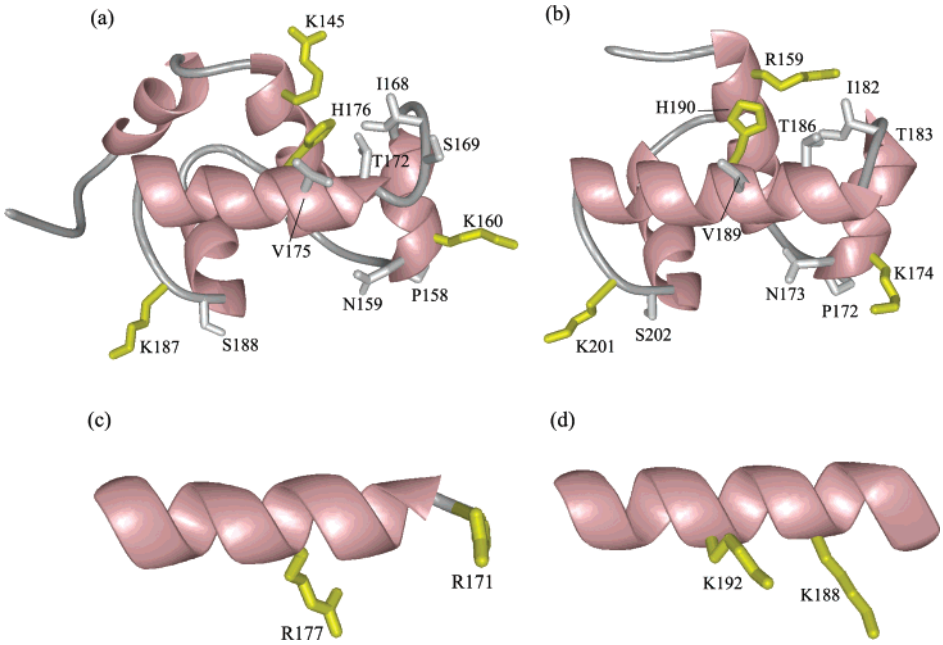

FIGURE 6: Putative residues involved in the DNA-binding activity of FixJC. Based on a structural comparison of FixJC with NarLC, the side-chain atoms of the conserved residues responsible for DNA recognition are shown in the ribbon representations of the FixJC (a) and NarLC (b) structures. Positively charged residues (Arg, Lys, and His) are colored yellow. Lys188 and Lys192 of NarLC (d), which are positioned on the recognition helix, were in contact with the major groove floor via their side chains in the NarLC−DNA complex. On the recognition helix of FixJC, two arginine residues, Arg171 and Arg177, are also present, but they are located at positions different from those of the two lysine residues of NarLC (c).

Table 2: DNA Binding Activity of FixJ Mutants[a]

WT	E144A	R145A	S169A	R171A	E174A	R177A
+	+	−	+	+	+	±

[a] FixJ proteins were phosphorylated with acetyl phosphate, and subjected to a *fixK* promoter binding assay.

recognition of the target DNAs. Indeed, the α4 mutants, R171A and E174A, were devoid of *fixK* DNA binding activity (Table 2).

FixJC contains an extra helix in the N-terminus (α1), Ile135 and Leu139, which provide for a hydrophobic interaction network with Val149/Leu150 of α2 and Ala196 of α5. Since the corresponding region of unphosphorylated NarL, which is the inactive form relative to DNA binding, is disordered in the crystals, the formation of α1 in FixJC may contribute to stabilize the overall structure of the C-terminal domain so that FixJC is able to bind to the target DNA. At present, however, the possibility that the domain truncation might artificially generate a helical structure cannot be excluded.

Analysis of the Interaction between FixJC and the fixK Promoter DNA. To elucidate the basic mechanism of the sequence-specific DNA recognition, we carried out NMR

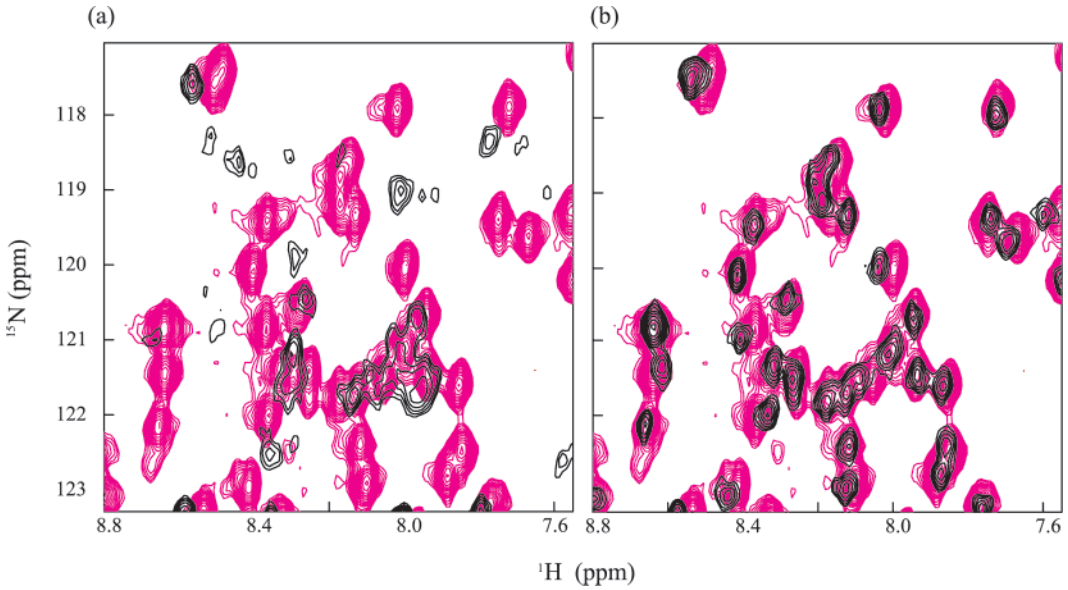

FIGURE 7: Overlays of the expansions of 2D ^{1}H−^{15}N HSQC spectra from the titration of ^{15}N-labeled FixJC with two unlabeled DNA fragments. One contains the specific binding site for FixJC (a), and the other does not (b). In both panels, the spectra in the presence of DNA at the molar ratio of FixJC:DNA = 2:1 are presented by black contours, while the spectrum of FixJC alone is plotted in red.

titration experiments of FixJC using two 21 bp synthetic double-stranded DNA fragments. One contains the FixJ recognition sequence from the *fixK* promoter identified in the present study, and the other contains the downstream region of the promoter and was used as a negative control.

The 2D ^{1}H−^{15}N HSQC spectra of ^{13}C/^{15}N-labeled FixJC showed drastic chemical shift changes and line broadening of the cross-peaks in the presence of the target DNA (Figure 7a), while the addition of the negative control caused negligible effects (Figure 7b). These spectral perturbations suggested that the binding of FixJC to its recognition sequence occurs via an intermediate to slow exchange on the NMR time scale, while the interaction with the unrelated sequence is in a much faster exchange regime. Differences in the NMR titration experiments presumably reflect the different binding affinities for the two DNAs.

It is noteworthy that, in addition to the extreme line broadening of cross-peaks, more than 30 new broad cross-peaks were observed in 2D ^{1}H−^{15}N HSQC when more than a half-fold molar excess of the target DNA was added, suggesting that more than one molecule of FixJC binds to the target DNA. This is consistent with the fact that phosphorylated FixJ dimer binds to the *fixK* promoter (*6*, *11*).

DISCUSSION

The FixL/FixJ system directs the expression of nitrogen fixation related genes under oxygen-limited conditions in *Sinorhizobium meliloti*. Upon phosphorylation, FixJ is converted into an active transcriptional factor for the *fixK* and *nifA* genes. However, their promoter regions do not share a sequence similarity (*10*), suggesting that two distinct binding modes are involved. To understand how FixJ binds to the *fixK* promoter, we first identified the recognition sequence of the high affinity binding site in the *fixK* promoter by a binding assay using native and mutated DNAs. We then determined the structure of the C-terminal DNA binding domain of FixJ and analyzed the interaction between the FixJC protein and the target DNA.

Regardless of whether or not response regulators are dimerized upon phosphorylation, their target DNAs usually contain direct repeats (*9*, *34*, *40*) or inverted repeats (*8*, *37*) for the accommodation of two protein molecules. However, the high affinity target region of the *fixK* promoter is thought to contain neither significant palindromic nor tandem structures, and the recognition sequences remain elusive (*4*). The present mutational scanning experiment unambiguously indicated that 5′-T$_{-65}$AAGTAATTTCCCTTA$_{-50}$-3′ is indispensable for maximal FixJ binding (Figure 2). The 16 bp sequence is sufficiently long for the binding of dimeric FixJ, because a 5−7 bp sequence is required to accommodate one molecule of the HTH structure of DNA binding proteins (*41*). The short inverted repeats T$_{-65}$AAG$_{-62}$ and C$_{-53}$TTA$_{-50}$ are present, but the latter appears to make only a minor contribution (Figure 2). This is consistent with the SELEX experiment, indicating that FixJ−P preferentially binds to 5′-tctaaGTAGTTTCCC-3′ (lower cases are the default sequence contiguous to random nucleotides in the DNA pool) and T$_{-52}$TA$_{-50}$ has not been selected (*42*). Furthermore, although the sequence of the promoter region of *Mesorhizobium loti* is the most similar to that of *S. meliloti*, such an inverted repeat is partially disrupted (Figure 2).

The present structural model confirmed that FixJC consists of five α-helices and possesses a HTH motif which is preferred for sequence-specific DNA binding by bacterial transcriptional factors (*41*). In particular, the overall structure is very similar to that of the C-terminal domains of NarL and Spo0A (Figure 5).

As mentioned in the Results section, the structures of DNA-bound complexes of NarLC and other DNA binding proteins have shown that several residues around the recognition helix participate in nonspecific binding to the phosphate backbone, in addition to the sequence-specific binding of some residues of the recognition helix (α9 of NarLC) to the floor of the major DNA groove. Many of these are positively charged and appear to interact with the negatively charged phosphate backbones of DNA. Interestingly, these residues for nonspecific binding are well

conserved in FixJ (Figures 1 and 6a). Therefore, these structural similarities predict that the α4 residues of FixJC function in sequence-specific DNA recognition, and the surrounding residues comprise a scaffold for nonspecific binding. Thus, one can consider that the difference in the primary sequence of the recognition helix between FixJ and NarL enables them to specifically bind to each cognate DNA. Indeed, in the NarLC−DNA complex structure, two positively charged residues, Lys188 and Lys192, which are not conserved between NarLC and FixJC, are reported to come into contact with the major groove floor (Figure 6d). In the recognition helix of FixJC, instead, two arginine residues, Arg171 and Arg177, are found at different positions (Figure 6c). These two arginine residues are the most likely candidates for carrying out the sequence-specific binding of FixJC.

Interactions between FixJC and the *fixK* promoter were observed by means of NMR titration experiments. However, we were unable to identify the individual amino acids involved in the specific binding to the DNA, because the assignments were completed poorly for the following reasons: The NMR spectra exhibited a mixture of many missing cross-peaks and extreme line broadening caused by an intermediate exchange reaction and newly born cross-peaks caused by a slow exchange reaction. These observations suggest that FixJC binds to DNA with the low binding affinity. This is consistent with a previous result indicating that the DNA binding affinity of FixJ−P is much lower than that of OmpR−P (*11*, *43*). Extreme chemical shift changes were observed when the molar ratio of the target DNA:FixJC reached 0.5:1 (1:2). The perturbation was almost saturated even when the ratio exceeded 0.5. These results suggest that more than one molecule of FixJC binds to the high affinity recognition sequence of the *fixK* promoter, consistent with previous studies, which showed that the phosphorylation-induced dimerization of FixJ is required for binding to the DNA (*6*, *11*). The nuclease protection assay showed that the *fixK* promoter contains the two overlapping binding sites (−69 to −44, −57 to −31) (*4*). The −69 to −44 region serves as a high affinity binding site, and the downstream region has a low affinity for FixJ. It is, therefore, most likely that the high affinity binding site is responsible for the FixL/FixJ-linked transcriptional regulatory function. Our NMR titration analysis using the −49 to −29 DNA indicated a nonspecific interaction, since the low affinity region is truncated.

Therefore, two molecules of FixJC, in dimeric form, appear to bind to the *fixK* DNA with different affinities, since the recognition sequence is necessary and sufficient in length for the accommodation of two FixJC molecules. This is in agreement with previous data showing that the 15 bp target region is protected against DNase by binding of the FixJ−P dimer (*42*).

The response regulator family displays a diversity of phosphorylation-induced dimerization, topology of protein molecules aligned on DNA, and DNA binding affinity although they share an overall structural similarity. NarLC is dimerized in a tail-to-tail manner on the bent *nirB* promoter with inverted repeats, although the phosphorylation-induced dimerization of the full-length protein has not been detected in solution (*8*). Spo0AC binds to the *abrB* promoter in a head-to-tail manner, and the receiver domain is unequivocally responsible for the phosphorylation-induced dimerization (*9*). Such head-to-tail binding has been proposed for OmpR and PhoB, whose targets contain direct repeats (*34*, *45*). In the case of PhoB, phosphorylation-induced dimerization has been reported (*46*). Determination of the DNA-interacting residues seems to owe their high affinity for the target DNA (their K_d values are submicromolar) (*34*, *43*). In spite of failure to identify the DNA-interacting amino acid residues of FixJ due to the low binding affinity, the present NMR titration experiments rather provided the information of two-molecule binding with different affinities. The first binding of the FixJC monomer to the *fixK* promoter may induce conformational changes in DNA bending and/or a structural change in FixJC, thus enhancing the affinity for a second molecule. As a result, the dimerization interface between the two molecules might be stabilized when bound to the DNA, although the truncated DNA binding domains are not dimerized solely. When considering the significance of the dimer formation of FixJ−P, one can imagine that the second FixJ molecule might play a role in interaction with RNA polymerase subunit(s) to recruit the enzyme to the *fixK* promoter (*47*). In contrast, the recognition sequence of the *nifA* promoter is a GTA(C/A)GTAG octamer. Then, one subunit of the FixJ−P dimer appears to bind to the target sequence, and the aberrant binding might result in the expansion (∼40 bp) of the protected region by the DNase protection assay (*42*). The reason for the variety of DNA binding affinities of response regulators is still unknown. However, the long lifetime of FixJ−P might compensate its low binding affinity to function as an active transcriptional factor, whereas the phosphorylated forms of other response regulators have shorter lifetimes of the phosphoryl bond (*5*).

Phosphorylation-linked regulatory mechanisms still remain to be addressed. It has been suggested that the N-terminal regulator domain inhibits the transcriptional activity of the C-terminal domain in the unphosphorylated full-length FixJ (*3*, *4*). A crystallographic analysis of unphosphorylated NarL has provided plausible evidence that the N-terminal phosphoryl receiver domain masks the DNA binding surface of the C-terminal domain and the inhibitory interdomain interaction is eliminated upon phosphorylation (*32*, *34*). In contrast, the unphosphorylated DrrD and DrrB structures do not exhibit such steric hindrance, and the recognition helices are exposed to an aqueous phase, which does not account for the inability of DNA binding (*35*, *36*). Interestingly, the deduced structure of FixJ, obtained by low resolution small-angle X-ray scattering analysis, resembles unphosphorylated DrrD (*48*). The possibility that NarL and DrrD/FixJ employ different activation mechanisms and dimerization itself is important for DrrD/FixJ to bind to their target DNAs cannot be excluded. Because of this, structural differences between phosphorylated and unphosphorylated full-length FixJ should be elucidated.

SUPPORTING INFORMATION AVAILABLE

^{1}H, ^{13}C, and ^{15}N resonance assignments for the C-terminal domain of FixJ (FixJC). This material is available free of charge via the Internet at http://pubs.acs.org.

REFERENCES

1. David, M., Daveran, M.-L., Baut, J., Dedieu, A., Domergue, O., Ghai, J., Hertig, C., Boistard, P., and Kahn, D. (1988) Cascade

regulation of *nif* gene expression in *Rhizobium meliloti*, *Cell 54*, 671−683.
2. Gilles-Gonzalez, M. A., Ditta, G. S., and Helinski, D. R. (1991) A haemoprotein with kinase activity encoded by the oxygen sensor of *Rhizobium meliloti*, *Nature 350*, 170−172.
3. Da Re, S., Bertagnoli, S., Fourment, J., Reyrat, J. M., and Kahn, D. (1994) Intramolecular signal transduction within the FixJ transcriptional activator: in vitro evidence for the inhibitory effect of the phosphorylatable regulatory domain, *Nucleic Acids Res. 22*, 1555−1561.
4. Galinier, A., Garnerone, A. M., Reyrat, J. M., Kahn, D., Batut, J., and Boistard, P. (1994) Phosphorylation of the *Rhizobium meliloti* FixJ protein induces its binding to a compound regulatory region at the *fixK* promoter, *J. Biol. Chem. 269*, 23784−23789.
5. Birck, C., Mourey, L., Gouet, P., Fabry, B., Schumacher, J., Rousseau, P., Kahn, D., and Samama, J.-P. (1999) Conformational changes induced by phosphorylation of the FixJ receiver domain, *Struct. Fold Des. 7*, 1505−1515.
6. Da Re, S., Schumacher, J., Rousseau, P., Fourment, J., Ebel, C., and Kahn, D. (1999) Phosphorylation-induced dimerization of the FixJ receiver domain. *Mol. Microbiol. 34*, 504−511.
7. Gunsalus, R. P., Kalman, L. V., and Stewart, R. R. (1989) Nucleotide sequence of the narL gene that is involved in global regulation of nitrate controlled respiratory genes of Escherichia coli, *Nucleic Acids Res. 17*, 1965−1975.
8. Maris, A. E., Sawaya, M. R., Kaczor-Grzeskowiak, M., Jarvis, M. R., Bearson, S. M., Kopka, M. L., Schröder, I., Gunsalus, R. P., and Dickerson, R. E. (2002) Dimerization allows DNA target site recognition by the NarL response regulator, *Nat. Struct. Biol. 9*, 771−778.
9. Zhao, H., Msadek, T., Zapf, J., Madhusudan, Hoch, J. A., and Varughese, K. I. (2002) DNA complexed structure of the key transcription factor initiating development in sporulating bacteria, *Structure (Cambridge) 10*, 1041−1050.
10. Agron, P. G., Ditta, G. S., and Helinski, D. R. (1992) Mutational analysis of the Rhizobium meliloti nifA promoter, *J. Bacteriol. 174*, 4120−4129.
11. Saito, K.,Ito, E., Hosono, K., Nakamura, K., Imai, K., Iizuka, T., Shiro, Y., and Nakamura, H. (2003) The uncoupling of oxygen sensing, phosphorylation signaling and transcriptional activation in oxygen sensor FixL and FixJ mutants, *Mol. Microbiol. 48*, 373−383.
12. Laue, E. D., Mayger, M. R., Skilling, J., and Staunton, J. (1986) Reconstruction of phase sensitive 2D NMR spectra by maximum entropy, *J. Magn. Reson. 68*, 14−29.
13. Kraulis, P. J. (1989) Ansig-a program for the assignment of protein ^{1}H 2D-NMR spectra by interactive computer-graphics, *J. Magn. Reson. 84*, 627−633.
14. Grzesiek, S., and Bax, A. (1992) Correlating backbone amide and side chain resonances in larger proteins by multiple relayed triple resonance NMR, *J. Am. Chem. Soc. 114*, 6291−6293.
15. Grzesiek, S., and Bax, A. (1992) An Efficient experiment for sequential backbone assignment of medium-sized isotropically enriched proteins, *J. Magn. Reson. 99*, 201−207.
16. Clubb, R. T., Thanabal, V., and Wagner, G. (1992) A constant-time three-dimensional triple-resonance pulse scheme to correlate intraresidue $^{1}H^{N}$, ^{15}N and $^{13}C'$ chemical shifts in ^{15}N-^{13}C-labeled proteins, *J. Magn. Reson. 97*, 213−217.
17. Grzesiek, S., and Bax, A. (1993) Amino acid type determination in the sequential assignment procedure of uniformly ^{13}C/^{15}N-enriched proteins, *J. Biomol. NMR 3*, 185−204.
18. Clowes, R. T., Boucher, W., Hardman, C. H., Domaille, P. J., and Laue, E. D. (1993) A 4D HCC(CO)NNH experiment for the correlation of aliphatic side-chain and backbone resonances in ^{13}C/^{15}N-labelled proteins, *J. Biolmol. NMR 3*, 349−354.
19. Grzesiek, S., Anglister, J., and Bax, A. (1993) Correlation of backbone amide and aliphatic side-chain resonances in ^{13}C/^{15}N-enriched proteins by isotropic mixing of 13C magnetization, *J. Magn. Reson., Ser. B 101*, 114−119.
20. Bax, A., Clore, G. M., and Gronenborn, A. M. (1990) ^{1}H-^{1}H correlation via isotropic mixing of ^{13}C magnetization, a new three-dimensional approach for assigning ^{1}H and ^{13}C spectra of ^{13}C-enriched proteins, *J. Magn. Reson. 88*, 425−431.
21. Marion, D., Kay, L. E., Sparks, S. W., Torchica, D. A., and Bax, A. (1989) Three-dimensional heteronuclear NMR of ^{15}N-labelled proteins, *J. Am. Chem. Soc. 111*, 1515−1517.
22. Wishart, D. S., and Sykes, B. D. (1994) The ^{13}C Chemical-Shift Index: a simple method for the identification of protein secondary structure using ^{13}C chemical shift data, *J. Biomol. NMR 4*, 171−180.
23. Brunger, A. T., Adams, P. D., Clore, G. M., DeLano, W. L., Gros, P., Grosse-Kunstleve, R. W., Jiang, J. S., Kuszewski, J., Nilges, M., Pannu, N. S., Read, R. J., Rice, L. M., Simonson, T., and Warren, G. L. (1998) Crystallography & NMR system: A new software suite for macromolecular structure determination, *Acta Crystallogr. D54*, 905−921.
24. Laskowski, R. A., Rullmann, J. A. C., MacArthur, M. W., Kaptein, R., and Thornton, J. M., (1996) AQUA and PROCHECK-NMR: programs for checking the quality of protein structures solved by NMR, *J. Biomol. NMR 8*, 477−486.
25. Williamson, M. P. and Asakura, T. (1993) Enpirical comparisons of models for chemical-shift calculation in proteins, *J. Magn. Reson., Ser. B 101*, 63−71.
26. Williamson, M. P., Kikuchi, J., and Asakura, T. (1995) Application of ^{1}H NMR chemical shifts to measure the quality of protein structures, *J. Mol. Biol. 247*, 541−546.
27. Bodenhausen, G., and Ruden, D. J. (1980) Natural abundance nitrogen-15 NMR by enhanced heteronuclear spectroscopy, *Chem. Phys. Lett. 69*, 185−189.
28. Grzesiek, S., and Bax, A. (1993) The importance of not saturating H_2O in protein NMR. Application to sensitivity enhancement and NOE measurements, *J. Am. Chem. Soc., 115*, 12593−12594.
29. Ikura, M., Kay, L. E., and Bax, A. (1990) A novel approach for sequential of ^{1}H, ^{13}C, and ^{15}N spectra of proteins: heteronuclear triple-resonance three-dimensional NMR spectroscopy. Application to calmodulin, *Biochemistry 29*, 4659−4667.
30. Fischer, H.-M. (1994) Genetic regulation of nitrogen fixation in rhizobia, *Microbiol. Rev. 58*, 352−386.
31. Nilges, M. (1995) Calculation of protein structure with ambiguous distance restraints. Automated assignment of ambiguous NOE crosspeaks and disulphide connections, *J. Mol. Biol. 245*, 645−660.
32. Baikalov, I., Schröder, I., Kaczor-Grzeskowiak, M., Grzeskowiak, K., Gunsalus, R. P., and Dickerson, R. E. (1996) Structure of the Escherichia coli response regulator NarL, *Biochemistry 35*, 11053−11061.
33. Martinez-Hackert, E., and Stock, A. M. (1997) The DNA-binding domain of OmpR: crystal structures of a winged helix, *Structure 5*, 109−124.
34. Okamura, H., Hanaoka, S., Nagadoi, A., Makino, K., and Nishimura, Y. (2000) Structural comparison of the PhoB and OmpR DNA-binding/transactivation domains and the arrangement of PhoB molecules on the phosphate box, *J. Mol. Biol. 295*, 1225−1236.
35. Buckler, D. R., Zhou, Y., and Stock, A. M. (2002) Evidence of intradomain and interdomain flexibility in an OmpR/PhoB homologue from *Thermotoga maritima*, *Structure (Cambridge) 10*, 153−164.
36. Robinson, V. L., Wu, T., and Stock, A. M. (2003) Structural analysis of the domain interface in DrrB, a response regulator of the OmpR/PhoB subfamily, *J. Bacteriol. 185*, 4186−4194.
37. Laguri, C., Phillips-Jones, M. K., Williamson, M. P. (2003) Solution structure and DNA binding of the effector domain from the global regulator PrrA (RegA) from Rhodobacter sphaeroides: insights into DNA binding specificity, *Nucleic Acids Res. 31*, 6778−6787.
38. Pristovsek, P., Sengupta, K., Löhr, F., Schäfer, B, von Trebra, M. W., Rüterjans, H., and Bernhard, F. (2003) Structural analysis of the DNA-binding domain of the Erwinia amylovora RcsB protein and its interaction with the RcsAB box, *J. Biol. Chem. 278*, 17752−17759.
39. Maris, A. E., Sawaya, M. R., Kaczor-Grzeskowiak, M., Jarvis, M. R., Bearson, S. M., Kopka, M. L., Schröder, I., Gunsalus, R. P., and Dickerson, R. E. (2002) Dimerization allows DNA target site recognition by the NarL response regulator, *Nat. Struct. Biol. 9*, 771−778.
40. Harrison-McMonagle, P., Denissova, N., Martinez-Hackert, E., Ebright, R. H., and Stock, A. M. (1999) Orientation of OmpR monomers within an OmpR:DNA complex determined by DNA affinity cleaving, *J. Mol. Biol. 285*, 555−566.
41. Pabo, C. O., and Sauer, R. T. (1992) Transcription factors: structural families and principles of DNA recognition, *Annu. Rev. Biochem. 61*, 1053−1095.
42. Ferrieres, L., and Kahn, D. (2002) Two distinct classes of FixJ binding sites defined by in vitro selection, *FEBS Lett. 517*, 185−189.

43. Tran, V. K., Oropeza, R., and Kenney, L. J.(2000) A single amino acid substitution in the C terminus of OmpR alters DNA recognition and phosphorylation, *J. Mol. Biol. 299*, 1257−1270.
44. Eldridge, A. M., Kang, H. S., Johnson, E., Gunsalus, R., and Dahlquist, F. W. (2002) Effect of phosphorylation on the interdomain interaction of the response regulator, NarL, *Biochemistry 41*, 15173−15180.
45. Maris, A. E., Walthers, D., Mattison, K., Byers, N., and Kenney, L. J. (2005) The response regulator OmpR oligomerizes via β-sheets to form head-to-head dimers, *J. Mol. Biol. 350*, 843−856.
46. McCleary, W. R. (1996) The activation of PhoB by acetylphosphate, *Mol. Microbiol. 20*, 1155−1163.
47. Ton-Hoang, B., Salhi, M., Schumacher, J, Da Re, S., and Kahn, D. (2001) Promoter-specific involvement of the FixJ receiver domain in transcriptional activation, *J. Mol Biol. 312*, 583−589.
48. Birck, C., Malfois, M., Svergun, D., and Samama, J. (2002) Insights into signal transduction revealed by the low resolution structure of the FixJ response regulator, *J. Mol. Biol. 321*, 447−457.

BI0509043